

Design and Synthesis of Novel 1a,3,4-Oxadiazole Derivatives as Cytotoxic Agents: A Combined Experimental and Docking Study

P. Perla^{a,b}, N. Seelam^{a,*}, and R. Bera^b

^a Department of Chemistry, Koneru Lakshmaiah Education Foundation, Green Fields, Vaddeswaram, 522502 India

^b United States Pharmacopeia India Pvt. Ltd., IKP Knowledge Park, Genome Valley, Turkapally Village, Hyderabad, 500101 India

*e-mail: pullaraoperla.klu@gmail.com

Received August 19, 2019; revised October 11, 2019; accepted December 20, 2019

Abstract—A novel series of 3,5-disubstituted-1a,3,4-oxadiazole derivatives was synthesized and screened for in vitro anticancer activity. The newly synthesized compounds were characterized by ¹H, ¹³C NMR, IR spectroscopy and mass spectrometry. Among all the synthesized compounds, Oxaprozin derivatives containing 1,3,4-oxadiazole ring with 4-fluorobenzyl, 4-methoxybenzyl, methyl, and butyl substituents showed promising anticancer activity against HTB-57 cancer cell line, and derivatives with 4-fluorobenzyl, 4-methoxybenzyl, and propyl substituents exhibited a higher anticancer activity against a PPC-1 cell line. The possible binding mode interactions of the synthesized compounds with the key active site of the proline rich tyrosine kinase 2 Pyk2 receptor (PDB ID: 5TO8) were investigated using the AutoDock 4.2 docking protocol to find that the 1,3,4-oxadiazole Oxaprozin derivatives with methyl, ethyl, and propyl substituents had the highest binding energies ($\Delta G = -7.8, -7.6, \text{ and } -6.8$ kcal/mol, respectively) with Glu441, Leu431, Ala455, Val487, Met502, Leu556, Lys457, and Glu509.

Keywords: oxaprozin, 1,3,4-oxadiazole, anticancer activity, molecular docking, 5TO8

DOI: 10.1134/S1070428020050280

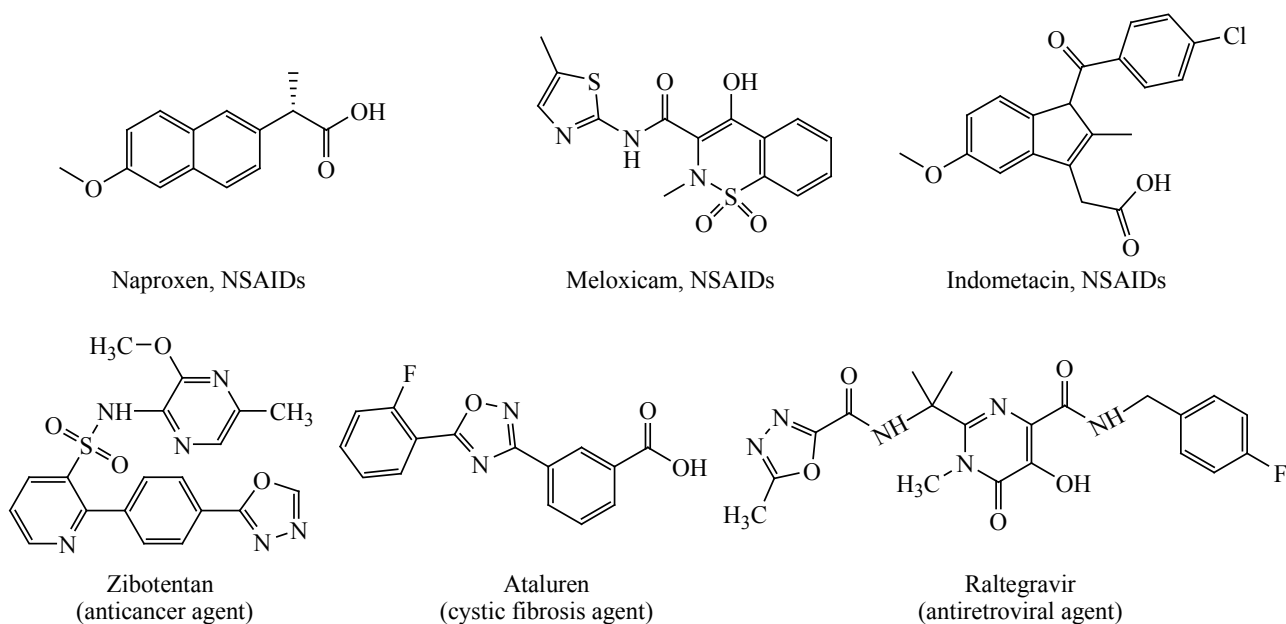
INTRODUCTION

Cancer remains the second major challenging medical disorder among the causes of morbidity and mortality worldwide. However, the existing chemotherapy regimens are unsuccessful to meet the expectations and lead to unsatisfactory results [1]. According to the WHO estimates, about 17.1 million new cases and 9.6 million death cases related to cancer were registered in 2018 [2]. Hence, there is a clinical urgency for addressing these issues and generating suitable candidates with newer modes of action and fewer or no side effects for cancer therapy. In view of the wide prevalence of multidrug-resistant Gram-positive and Gram-negative pathogenic bacteria that cause life-threatening infections in living organisms, thereby forming acquired resistance to many existing drugs, the desperate need in miracle agents [3] to treat such infections becomes even more obvious.

The 1,3,4-oxadiazole pharmacophore has gained much attention over the past years due to its broad-

spectrum biological activity profiles [4] owing to the presence of an NCO oxophoric linkage. Several methods for facile construction of the oxadiazole scaffold have been developed [5]. Symmetrically and unsymmetrically 2,5-disubstituted oxadiazole derivatives have been encompassed with promising pharmacological profiles, such as antitubercular [6], antimicrobial [7], anticancer [8], antiepileptic [9], antifungal [10], analgesic [11], antitumor [12], etc. Compounds comprising oxadiazole as a core nucleus are in late stages of clinical trials, for example, Zibotentan, Ataluren and Raltegravir, or are already used as important non-steroidal anti-inflammatory drugs (NSAIDs), for example Naproxen, Meloxicam, and Indometacin. Some oxadiazoles are very good bioisosteres of esters and amides, which ensures stronger hydrogen bonding with different receptors and, as a result, much enhancing biological responses. On the other hand, the therapeutic use of Oxaprozin [3-(4,5-diphenyl-1,3-oxazol-2-yl)propanoic acid], one of the leading NSAIDs in the global clinical market,

Scheme 1.



is restricted by its side effects, such as gastrointestinal injury (GI), peptic ulceration, and perforation, developing due to the presence of the corrosive carboxylic group, as well as considerable damage to the renal system [13] (Scheme 1).

As part of our work on the identification of dormant heterocyclic scaffolds, we have designed the synthesis of hybrid template **6**, starting from Oxaprozin (Scheme 2). To mask the potential side effects of the carboxylic motif of Oxaprozin, we obtained its 1,3,4-oxadiazole bio-isostere for safer profiles. Different substituents were introduced in the other vacant position of the oxadiazole ring via C–N bond formation, which was expected to enhance the lipophilicity of the resulting derivatives and improve their pharmacokinetic properties by facilitating penetration into the cell wall.

The aim of this work was to combine the oxaprozin and 1,3,4-oxadiazole rings in one compact structure for the purpose of synergism. We also extended our effort to a molecular docking study of this biologically interesting, from the viewpoint of anticancer activity, class of compounds [14].

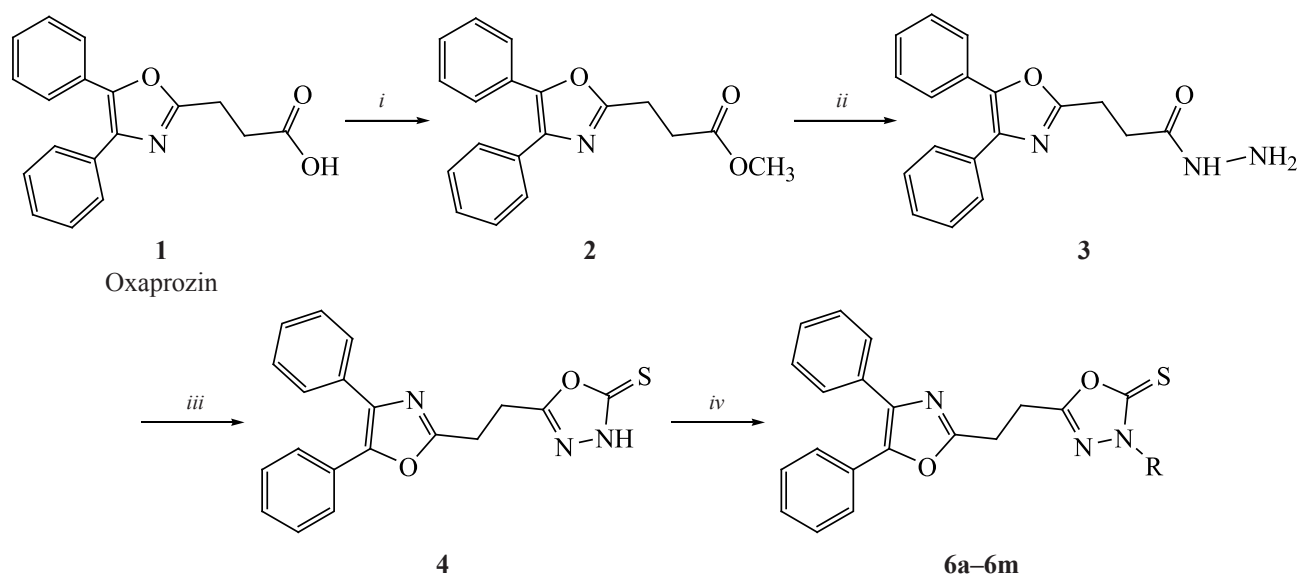
RESULTS AND DISCUSSION

The hitherto unknown 1,3,4-oxadiazole derivatives of Oxaprozin were synthesized by conventional methods (Scheme 2). Ester **2** was prepared by refluxing its acid precursor with methanol for 8 h in the presence

of H_2SO_4 as a catalyst. The subsequent hydrazinolysis of compound **2** with 100% hydrazine hydrate in methanol under reflux provided hydrazide **3** [15]. The intermolecular cyclization of the latter with CS_2 in boiling ethanol under strongly basic conditions gave the key 1,3,4-oxadiazole intermediate **4** in a good yield. Finally, compound **4** was reacted with electrophilic halides **5a–5m** in K_2CO_3 at ambient temperature for 7–9 h to obtain the corresponding target products **6a–6m** in excellent yields.

The compositions and structures of the synthesized compounds were confirmed by elemental analysis, IR, ^1H and ^{13}C NMR spectroscopy, and mass spectrometry. The ^1H NMR spectrum of compound **6a** displays signals at δ 11.31 ppm (NH) and 7.62–7.27 ppm (aromatic protons). The ^{13}C NMR spectrum of compound **6a** showed signals at δ_{C} 162.63 (C^2) and 155.84 ppm (C^5), providing evidence for the presence of the 1,3,4-oxadiazole core, as well as at δ_{C} 141.02–121.77 ppm (aromatic carbons). The IR spectrum of **6a** contained stretching absorption bands at 1483 [$\nu(\text{C}=\text{N})$], 1581 [$\nu(\text{C}=\text{C})$], and 1152 and 1052 cm^{-1} [$\nu(\text{C}-\text{O}-\text{C})$]. The latter two bands are assignable to the C–O–C linkages in the oxadiazole and oxazole rings. The mass spectrum displayed a molecular ion peak at m/z 440.6 [$M + 1$] $^+$, which confirmed the molecular weight of 3-benzyl-5-[2-(4,5-diphenyloxazol-2-yl)ethyl]-1,3,4-oxadiazole-2(3*H*)-thione.

Scheme 2.



i, CH₃OH, H₂SO₄, reflux, 7 h; *ii*, NH₂NH₂·H₂O, CH₃OH, reflux, 8 h;
iii, EtOH, KOH, CS₂, reflux, 9 h; *iv*, RX (**5a–5m**), K₂CO₃, DMF, rt, 7–9 h.

5, 6, R = PhCH₂ (**a**), *p*-FC₆H₄CH₂ (**b**), *p*-PhCH₂OC₆H₄CH₂ (**c**), *p*-MeOC₆H₄CH₂ (**d**),
p-ClC₆H₄CH₂ (**e**), Me (**f**), Et (**g**), Pr (**h**), Bu (**i**), octyl (**j**), isobutyl (**k**), allyl (**l**), propargyl (**m**); **5**, X = F, Cl.

Anticancer activity testing. In vitro cytotoxicity of compounds **6** was assessed using MTT colorimetric assay according to the ATCC protocol at 25 μM against the PPC-1 prostate adenocarcinoma and HTB-57 lung adenocarcinoma cell lines. Doxorubicin (DXN) was used as reference. The resulting data are listed in Table 1. As seen from the table 1, all the test compounds, except for **6k**, demonstrated a higher activity than the reference compound against both cancer cell lines. It was found that HTB-57 cells were more sensitive to the test compounds than PPC-1 cells. Compound **6d** displayed promising activity and compounds **6b**, **6f**, and **6i** demonstrated moderate to good activity against the HTB-57 cell line. Compounds **6d**, **6h**, and **6b** showed the highest percentage inhibitions of 52.61, 41.65, and 34.76%, respectively. Among the derivatives with electron-donor groups, the activity against the lung cancer cell line decreased in the series **6d** (4-methoxybenzyl) > **6f** (methyl) > **6b** (4-fluorobenzyl) > **6i** (butyl), and the activity against the prostate cell line decreased in the series **6d** (4-methoxybenzyl) > **6h** (propyl) > **6b** (4-fluorobenzyl). The introduction of unsaturation, specifically compounds **6l** (allyl) and **6m** (propargyl), decreased activity against both the test cell lines.

Molecular docking study. The synthesized oxadiazoles **6a–6m** were identified as potent anticancer agents, and, therefore, we considered it of interest to employ molecular docking to simulate their interactions with the catalytic domain of the proline-rich tyrosine kinase 2Pyk2 and find the best binding conformations [16]. The results of molecular docking simulation for all the synthesized compounds are summarized in Table 2. Three- and two-dimensional representations of bonds between the protein and ligands are depicted in Fig. 1. The amino acid residues Gly434, Phe435, Phe436, Glu441, Lys457, Phe471, Glu508, Leu431, Ala455, Val487 and Leu556 and Asp567 of the protein 5TO8 are involved in H-bonding and hydrophobic interactions with almost all the ligand molecules. Ligands **6f**, **6d**, and **6h** showed the highest percentage inhibitions (Table 1) and docking score binding energies (Table 2) as compared to the other ligands.

The docking results indicate that compounds **6a–6m** are held in the active pocket by a combination of hydrophobic and van der Waals interactions with the catalytic site of the 5TO8 protein. Compounds **6f**, **6g**, **6h**, and **6m** displayed the highest binding energies ($\Delta G = -7.8, -7.6, -6.8,$ and -6.5 kcal/mol, respectively), whereas **6e**, **6i** and **6j** exhibited mediocre scores. Figu-

Table 1. In vitro cytotoxicity and physicochemical properties ($\log p/C\log p$) of compounds **6a–6m** by the MTT colorimetric assay

Compound no.	Percentage inhibition (%) at 25 μ M		$\log p/C\log p$
	PPC-1	HTB-57	
6a	23.63	17.23	6.3/5.95
6b	34.76	44.32	6.45/6.09
6c	31.70	33.32	7.9/7.64
6d	52.61	64.24	6.17/5.87
6e	22.06	24.28	6.85/6.66
6f	20.31	45.72	4.56/4.18
6g	9.32	21.20	4.9/4.71
6h	41.65	32.65	5.39/5.24
6i	30.58	43.68	5.81/5.77
6j	17.45	21.20	7.47/7.89
6k	6.70	9.28	5.79/5.64
6l	14.46	23.17	5.26/4.96
6m	22.46	18.64	4.78/4.28
Doxorubicin	60.12	49.08	Not determined

Table 2. Molecular docking results for the synthesized molecules docked into the chemokine receptor 5TO8

Ligand no.	Docking score binding energies ΔG (kcal/mol)	H-bonding	π - π interactions
6a	-4.9	–	Trp94, His113
6b	-5.4	Gln200	His113
6c	-5.5	Tyr190	Trp94, His113, Tyr116
6d	-6.3	Gln200	His113
6e	-5.1	Tyr190, Leu556	Trp94, His113, Tyr116
6f	-7.8	Leu431, Leu556	Ala455, Val487
6g	-7.6	Leu431, Phe435, Val439	Leu431, Glu509, Val439
6h	-6.8	Gln200	Trp94, Tyr116, His203
6i	-6.3	Trp591, Glu509	His113, His203
6j	-6.0	Gln200, Tyr255	Trp94, His203
6k	-4.6	Leu504, Asp567	His113, His203
6l	-5.8	–	Tyr116, His203
6m	-6.5	Gly434, Phe568	Lys457, Asp567, Phe568
Doxorubicin	-6.6	Tyr121, Gln200	Trp94

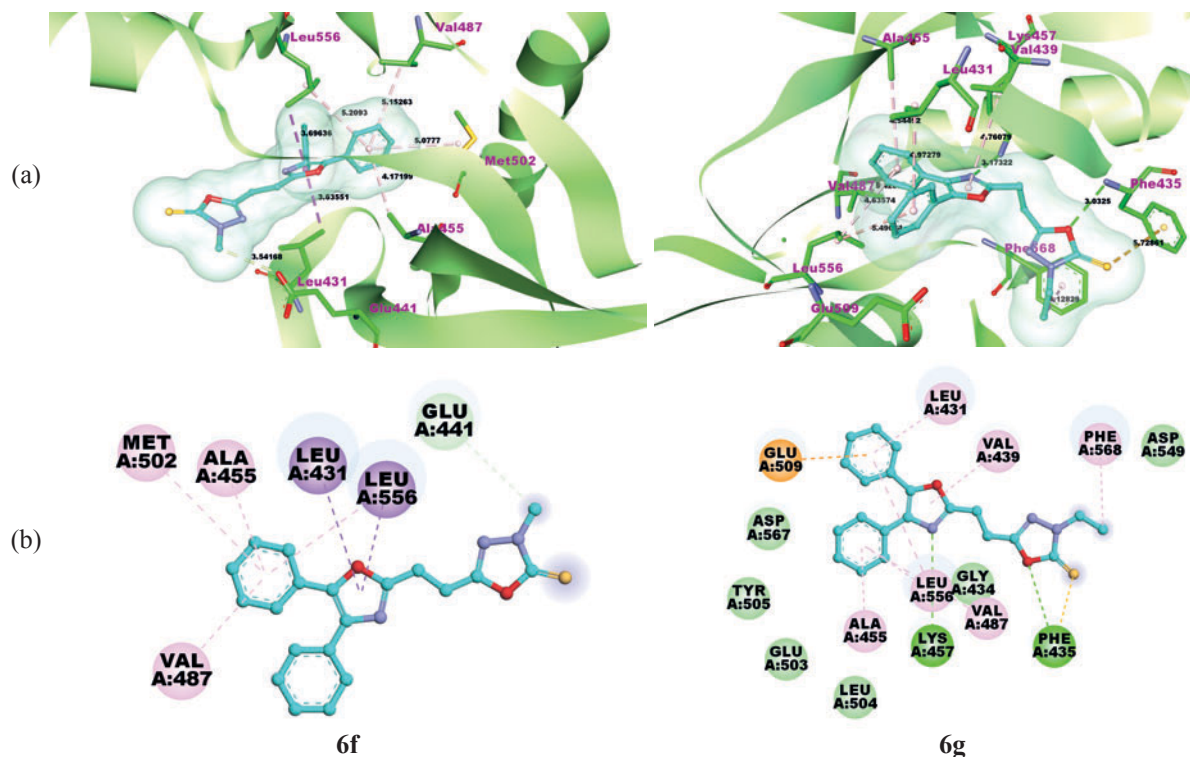


Fig. 1. (a) Autodock 3D representation of the docking interactions in the catalytic site of the 5TO8 protein: superimposition of the (thick tubes) co-crystallized native ligands and (balls and sticks) best docked poses of compounds **6f** and **6g**. Hydrogen bonds are shown by violet (**6f**) and light green dashed lines (**6g**) and π - π -stacking interactions are shown by light ash-colored (**6f**) and light yellow dashed lines (**6g**). (b) Autodock 2D representation of the hypothetical binding modes of compounds **6f** and **6g** in the active site of Pyk2.

re 1 demonstrates the predicted binding modes and detailed protein–inhibitor interactions of compounds **6f** and **6g** with the receptor. For compound **6f**, H-bonding with Leu431 (2.37 Å) and Leu556 (2.52 Å) and π - π stacking with Ala455 and Val487 were found. Compound **6m** showed a high docking score with the target receptor. The oxadiazole nitrogen interacts with the side chain of Gly434 (3.82 Å), and the oxadiazole ring shows π - π stacking with a hydrophobic residue Tyr116 and a polar residue His203. For ligand **6g**, interactions with the largest number of amino acids (Leu431, Phe435, Val439, Ala455, Lys457, Val487, Glu509, Phe568, and Leu556) with $\Delta G = -7.6$ kcal/mol were predicted. It was also found that the oxadiazole ring plays a key role in H-bonding with the catalytic site residues. The molecular docking results suggest that compounds **6f**, **6g**, **6h**, and **6m** have a potential to inhibit the proline-rich tyrosine kinase 2Pyk2 receptor 5TO8.

Molinspiration calculations. Further we performed a computational investigation of compounds **6a–6m** to predict their absorption, distribution, metabolism, and

excretion (ADME) properties using the Molinspiration online property calculation toolkit [17, 18]. The resulting data are listed in Table 3. Compounds **6a**, **6b**, **6c**, **6g**, and **6h** obeyed the Rule-of-Five, which implies their drug likeness. Compounds **6d–6f**, **6i**, **6j**, **6l**, and **6m** showed one violation and **6k**, two violations of the Rule-of-Five and, therefore, can be considered as moderately and poorly orally bioavailable, respectively. The result of this *in silico* ADME prediction analysis advocates that most of the synthesized compounds follow the computational assessment and thus represent a pharmacologically active frame for further potential hits.

EXPERIMENTAL

Materials and Instrumentation. All the chemicals were purchased from local suppliers and used without further purification. All reactions were carried in dry solvents under an inert atmosphere. The reaction progress was monitored by TLC on Merck Kieselgel 60 F₂₅₄ plates. Purification was performed by column chromatography on a Merck silica gel (100–200 mesh). The melting points were determined in open capillary

Table 3. Molinspiration molecular descriptors^a for structures **6a–6m**

Compound no.	miLog <i>P</i>	TPSA	% Abs	N atoms	MW	<i>n</i> _{ON}	<i>n</i> _{OHNH}	<i>n</i> violations	<i>N</i>	Volume, Å ³
6a	4.27	64.96	86.26	26	363.44	5	0	0	6	317.23
6b	4.64	64.96	86.26	27	377.47	5	0	0	7	334.03
6c	5.00	64.96	86.26	28	391.5	5	0	1	8	350.83
6d	5.70	64.96	86.26	29	405.52	5	0	1	9	367.63
6e	7.72	64.96	86.26	33	461.63	5	0	1	13	434.84
6f	5.39	64.96	86.26	29	405.52	5	0	1	8	367.42
6g	4.91	64.96	86.26	28	389.48	5	0	0	8	345.20
6h	4.42	64.96	86.26	28	387.46	5	0	0	7	339.73
6i	5.86	64.96	86.26	32	439.54	5	0	1	8	388.88
6j	6.02	64.96	86.26	33	457.53	5	0	1	8	393.81
6k	7.51	74.19	83.03	40	545.66	6	0	2	11	486.07
6l	5.92	74.19	83.03	34	469.57	6	0	1	9	414.42
6m	6.54	64.96	86.58	33	473.99	5	0	1	8	402.41
Oxaprozín	3.75	63.33	86.83	22	293.32	4	1	0	5	264.88

^a miLog *P*—Logarithm of *n*-octanol/water partition coefficient; %Abs—percentage absorption; TPSA—topological polar surface area; MW—molecular weight; *n*_{ON}—number of H-bond acceptors; *n*_{OHNH}—number of H-bond donors; *N*—number of rotatable bonds.

tubes on a Cintex melting point apparatus and are uncorrected. The IR spectra were recorded in KBr on a Perkin–Elmer 400 FTIR spectrometer or a Varian 670-IR FTIR spectrometer (ATR) in the frequency range of 600–4000 cm⁻¹. The ¹H and ¹³C NMR spectra were recorded in CDCl₃ and DMSO-*d*₆ on a Bruker DRX-300 (300 MHz FT NMR) or a Varian Mercury 500 MHz spectrometer. The ESI mass spectra were measured on a Jeol SX-102 spectrometer and high-resolution mass spectra (HRMS) were recorded on an Agilent Technologies 6510 Q-TOF spectrometer.

Cytotoxicity testing. The in vitro anticancer activity of the test compounds was tested using the MTT colorimetric assay [19, 20] as per the ATCC protocol. The cell lines used for testing included human prostate carcinoma–derived PPC-1 cells (ATCC no. CVCL-4778) and human lung adenocarcinoma–derived HBT-57 cells (ATCC no. SKLU1), which were procured from the American Type Culture Collection, Manassas, VA, USA. The lung cancer cell line HBT-57 was maintained in a DMEM medium containing 10% newborn calf serum (NBCS) along with 1% non-essential amino acids, 0.2% sodium bicarbonate, 1% sodium pyruvate

and 1% antibiotic mixture (10,000 U penicillin and 10 mg streptomycin per mL). The prostate cancer cell line PPC-1 was maintained in an RPMI-1640 medium containing 10% NBCS, 100 IU/mL penicillin, 100 mg/mL streptomycin, and 2 mM-glutamine. Cell lines were maintained at 37°C in a humidified 5% CO₂ incubator (Thermo Scientific) and processed by initial trypsinization to detach the adhered cells followed by centrifugation to obtain cell pellets. Fresh media were added to the pellets for cell counting on a haemocytometer, and 100 μL of the media with cells ranging from 5,000–6,000 per well were dispensed in a 96-well plate. The plate was incubated overnight in CO₂ incubator for the cells to adhere and regain its shape. After 24 h cells were treated with 25 μM solutions of the test compounds in the media. The cells were incubated for 48 h to assay the effect of the test compounds on the cell lines. A zero-hour reading with untreated cells and control with 1% DMSO were taken to subtract further from the 48 h reading. After 48 h incubation, the cells were treated with the MTT [(4,5-dimethylthiazol-2-yl)-2,5-diphenyltetrazolium bromide] dissolved in PBS (5 mg/mL) and incubated for 3–4 h at 37°C. The formazan crystals thus formed were dissolved in 100 μL

of DMSO, and the viability was measured at 540 nm on a Spectra Max multimode reader.

Molecular modeling. The ligands were sketched in Sybyl 6.7 and saved in the format of mol2 [21]. All the sketched molecules were converted to energy minimized 3D structures by using Gasteiger-Huckel charges for in silico protein–ligand docking using autodock Tools [22]. Each molecule was docked separately using Autodock 4.2 software. Initially the molecule was loaded, torsions were set and saved in PDBQT format. All the heteroatoms were removed from the 5TO8.PDB (crystal structure of macrocyclization of FAK inhibitors improves Pyk2 potency). After adding hydrogens, the model was saved in the PDBQT format, later ligands were prepared by optimizing the torsion angles and saved them in PDBQT format [23]. The PDB was also saved in PDBQT format. All calculations for protein-ligand flexible docking were performed using the Lamarckian Genetic Algorithm (LGA) method. A grid box with the dimensions of X: 15.137, Y: 17.850 and Z: -3.573 \AA , with a default grid spacing of 0.375 \AA was used. The best conformation was chosen with the lowest docked energy, after the docking search was completed. The interactions of pantothenate synthetase protein and ligand conformations, including hydrogen bonds and the bond lengths were analyzed.

Synthesis and Characterization. Methyl 3-(4,5-diphenyloxazol-2-yl)propanoate (2). To a solution of oxaprozin (2 g, 17 mmol) in methanol (15 mL), a few drops of conc. H_2SO_4 was added, and the resulting mixture was refluxed for 7 h. After completion of the reaction as indicated by TLC, excess methanol was distilled off. The residue was diluted with a 10% NaHCO_3 solution, the resulting solution was extracted with ethyl acetate, dried over Na_2SO_4 , and evaporated under a vacuum. The crude product was purified by recrystallization from ethanol to obtain 90% of compound **2** as a white solid, mp 57°C , R_f 0.48 (ethyl acetate–hexane, 20 : 80). IR spectrum, ν , cm^{-1} : 3049 [$\nu(\text{=CH})$], 2946, 3049 [$\nu(\text{CH})$], 1734, 3049 [$\nu(\text{C=O})$], 1590, 3049 [$\nu(\text{C=C})$], 1496 [$\nu(\text{C=N})$], 1060 [$\nu(\text{COC})$]. ^1H NMR spectrum (500 MHz, CDCl_3), δ , ppm: 2.92 t (2H, CH_2 , J 7.4 Hz), 3.20 t (2H, CH_2 , J 7.4 Hz), 3.74 s (3H, OCH_3), 7.26–7.38 m (6 H_{arom}), 7.56 d.d (2 H_{arom} , J 8.2 Hz), 7.64 d.d (2 H_{arom} , J 8.2 Hz). ^{13}C NMR spectrum (75 MHz, CDCl_3), δ , ppm: 23.03, 29.90, 60.87, 128.64, 128.97, 129.05, 132.07, 133.49, 136.05, 138.54, 145.07, 162.17, 173.02. Mass-spectrum, m/z : 308.0 [$M + 1$] $^+$.

3-(4,5-Diphenyloxazol-2-yl)propanehydrazide (3). To a solution of compound **2** (4.70 g, 15 mmol) in ethanol (50 mL), hydrazine hydrate (1.6 mL, 30 mmol) was added, and the mixture was refluxed for about 8 hr. Excess ethanol was distilled off, the residue was poured into water, and the resulting solution was extracted with ethyl acetate ($2 \times 30 \text{ mL}$). The combined organic extracts were dried over Na_2SO_4 and evaporated under a vacuum. The crude product was purified by recrystallization from ethanol to obtain 88% of compound **3** as white solid, mp 109°C , R_f 0.50 (ethyl acetate–hexane, 70 : 30). IR spectrum, ν , cm^{-1} : 3324, 3285 [$\nu(\text{NH}, \text{NH}_2)$], 3034 [$\nu(\text{=CH})$], 2921 [$\nu(\text{CH})$], 1659 [$\nu(\text{C=O})$], 1513 [$\nu(\text{C=C})$], 1437 [$\nu(\text{C=N})$], 1060 [$\nu(\text{COC})$]. ^1H NMR spectrum (500 MHz, CDCl_3), δ , ppm: 2.72 t (2H, CH_2 , J 7.4 Hz), 3.20 t (2H, CH_2 , J 7.4 Hz), 4.77 br.s (2H, NH_2), 4.72 br.s (1H, NH), 7.31–7.38 m (6 H_{arom}), 7.55 d.d (2 H_{arom} , J 8.2 Hz), 7.60 d.d (2 H_{arom} , J 8.2 Hz). ^{13}C NMR spectrum (100 MHz, CDCl_3), δ , ppm: 23.03, 29.90, 128.64, 128.97, 129.53, 130.07, 132.49, 135.05, 138.69, 145.05, 162.22, 175.36. Mass-spectrum, m/z : 308.0 [$M + 1$] $^+$.

5-[2-(4,5-Diphenyloxazol-2-yl)ethyl]-1,3,4-oxadiazole-2(3H)-thione (4). A mixture of compound **3** (4 g, 14 mmol), KOH (0.95 g, 16 mmol), and CS_2 (1.75 mL, 27 mmol) in ethanol (45 mL) was stirred under reflux for 9 h until H_2S no longer evolved. The progress of the reaction was monitored by TLC. The solvent was then distilled off, and the residue was poured over crushed ice, and the solution was acidified with 10% HCl until pH 5. The precipitated crude product was filtered off, washed with water, dried, and recrystallized from ethanol to obtain 85% of compound **4** as a white solid, mp 156°C , R_f 0.42 (ethyl acetate–hexane, 40 : 60). IR spectrum, ν , cm^{-1} : 3372 [$\nu(\text{NH})$], 3079 [$\nu(\text{=CH})$], 2914, 2766 [$\nu(\text{CH})$], 1621 [$\nu(\text{C=S})$], 1555, 1511 [$\nu(\text{C=C})$], 1435 [$\nu(\text{C=N})$], 1155 [$\nu(\text{COC})$]. ^1H NMR spectrum (500 MHz, CDCl_3), δ , ppm: 3.27–3.37 m (4H, CH_2CH_2), 7.26–7.38 m (6 H_{arom}), 7.55–7.63 m (4 H_{arom}), 11.31 br.s (1H, SH). ^{13}C NMR spectrum (75 MHz, CDCl_3), δ , ppm: 23.29, 24.09, 126.50, 128.05, 128.41, 128.74, 131.65, 135.09, 146.05, 160.51, 162.51. Mass-spectrum (ESI-MS), m/z : 350.0 [$M + 1$] $^+$.

Synthesis of compounds 6a–6m (general procedure). To a solution of compound **4** (1.0 equiv) in DMF (5 vol), substituted halide **5a–5m** (1.2 equiv) and K_2CO_3 carbonate (1.5 equiv) were added. The reaction mixture was stirred at ambient temperature for 7–9 h,

diluted with water, and extracted with ethyl acetate (2 × 20 mL). The crude product was purified by column chromatography. Compounds **6a–6m** were obtained in yields of 63–87% and characterized by ¹H and ¹³C NMR spectroscopy, mass spectrometry, and elemental analysis.

3-Benzyl-5-[2-(4,5-diphenyloxazol-2-yl)ethyl]-1,3,4-oxadiazole-2(3H)-thione (6a). Light brown solid, mp 90°C, *R_f* 0.46 (ethyl acetate–hexane, 30 : 70). IR spectrum, ν , cm⁻¹: 3057, 3029 [ν (=CH)], 2920, 2848 [ν (CH)], 1614 [ν (C=S)], 1588 [ν (C=C)], 1495 [ν (C=N)], 1440 [ν (CN)], 1221, 1155 [ν (COC)]. ¹H NMR spectrum (500 MHz, CDCl₃), δ , ppm: 3.34–3.29 m (4H, CH₂), 4.77 s (2H, NCH₂), 7.36–7.26 m (6H_{arom}), 7.57 d.d (2H_{arom}, *J* 8.8 Hz), 7.62 d.d (2H_{arom}, *J* 8.8 Hz). ¹³C NMR spectrum (125 MHz, CDCl₃), δ , ppm: 18.28, 20.23, 32.02, 121.77, 123.15, 123.34, 123.42, 123.86, 123.94, 124.05, 124.37, 127.53, 130.74, 141.02, 155.84, 161.63. Mass-spectrum, *m/z*: 440 [*M* + 1]⁺. Found, %: C 71.05; H 4.82; N 9.56; S 7.30. C₂₆H₂₁N₃O₂S. Calculated, %: C 71.15; H 4.70; N 9.16; S 7.25.

5-[2-(4,5-Diphenyloxazol-2-yl)ethyl]-3-(4-fluorobenzyl)-1,3,4-oxadiazole-2(3H)-thione (6b). White solid, mp 76°C, *R_f* 0.43 (ethyl acetate–hexane, 30 : 70). IR spectrum, ν , cm⁻¹: 3040 [ν (=CH)], 2914, 2848 [ν (CH)], 1692 [ν (C=S)], 1577, 1500 [ν (C=C)], 1478 [ν (C=N)], 1232 [ν (CN)], 1232 [ν (COC)], 1150 [ν (COC)], 952 [ν (CF)]. ¹H NMR spectrum (500 MHz, CDCl₃), δ , ppm: 2.08–2.19 m (4H, CH₂), 3.21 s (2H, NCH₂), 6.03–6.19 m (10H_{arom}), 6.36 d.d (2H_{arom}, *J* 8.2 Hz), 6.45 d.d (2H_{arom}, *J* 8.2 Hz). ¹³C NMR spectrum (75 MHz, CDCl₃), δ , ppm: 23.02, 24.95, 35.94, 115.63, 115.80, 126.51, 127.90, 128.19, 128.61, 128.69, 128.76, 130.83, 130.90. Mass-spectrum, *m/z*: 457.2 [*M*]⁺, 456.1 [*M* – 1]⁺. Found, %: C 68.38; H 4.25; F 4.34; N 9.20; S 7.10. C₂₆H₂₀FN₃O₂S. Calculated, %: C 68.25; H 4.41; F 4.15; N 9.18; S 7.01.

3-[4-(Benzyloxy)benzyl]-5-[2-(4,5-diphenyloxazol-2-yl)ethyl]-1,3,4-oxadiazole-2(3H)-thione (6c). White solid, mp 91°C, *R_f* 0.43 (ethyl acetate–hexane, 30 : 70). IR spectrum, ν , cm⁻¹: 3047 [ν (=CH)], 2925, 2854 [ν (CH)], 1578 [ν (C=C)], 1484 [ν (C=N)], 1247, 1029 [ν (COC)]. ¹H NMR spectrum (400 MHz, CDCl₃), δ , ppm: 3.45–3.30 m (4H, CH₂), 4.40 s (2H, NCH₂), 5.03 s (2H, OCH₂), 6.91 d (2H_{arom}, *J* 8.5 Hz), 7.48–7.27 m (13H_{arom}), 7.56 d.d (2H_{arom}, *J* 8.2 Hz), 7.62 d.d (2H_{arom}, *J* 8.2 Hz). ¹³C NMR spectrum

(100 MHz, CDCl₃), δ , ppm: 22.94, 24.91, 36.34, 69.96, 115.01, 126.44, 127.38, 127.59, 127.81, 127.95, 128.08, 128.53, 128.60, 128.70, 130.33, 132.20, 135.15, 136.69, 145.68, 158.54, 160.53, 164.26, 166.23. Mass-spectrum, *m/z*: 546.0 [*M* + 1]⁺. Found, %: C 72.01; H 4.72; N 7.55; S 5.12. C₃₃H₂₇N₃O₃S. Calculated, %: C 72.64; H 4.99; N 7.70; S 5.88.

5-[2-(4,5-Diphenyloxazol-2-yl)ethyl]-3-(4-methoxybenzyl)-1,3,4-oxadiazole-2(3H)-thione (6d). Light yellow solid, mp 88°C, *R_f* 0.43 (ethyl acetate–hexane, 30 : 70). IR spectrum, ν , cm⁻¹: 3043 [ν (=CH)], 2925, 2849 [ν (CH)], 1575 [ν (C=C)], 1473 [ν (C=N)], 1146, 1060 [ν (COC)]. ¹H NMR spectrum (500 MHz, CDCl₃), δ , ppm: 3.45–3.30 m (4H, CH₂), 3.90 s (3H, OCH₃), 5.12 s (2H, NCH₂), 6.61 d (2H_{arom}, *J* 8.5 Hz), 7.45–7.31 m (8H_{arom}), 7.56 d.d (2H_{arom}, *J* 8.2 Hz), 7.62 d.d (2H_{arom}, *J* 8.2 Hz). ¹³C NMR spectrum (125 MHz, CDCl₃), δ , ppm: 23.02, 24.99, 36.41, 55.30, 114.17, 126.51, 127.37, 127.90, 128.18, 128.62, 128.69, 128.77, 130.40, 132.27, 135.28, 145.77, 159.41, 160.62, 164.39, 166.32. Mass-spectrum, *m/z*: 470.15 [*M*]⁺, 470.15 [*M* + 1]⁺. Found, %: C 68.45; H 5.04; N 9.02; S 6.72. C₂₇H₂₃N₃O₃S. Calculated, %: C 69.06; H 4.94; N 8.95; S 6.83.

3-(4-Chlorobenzyl)-5-[2-(4,5-diphenyloxazol-2-yl)ethyl]-1,3,4-oxadiazole-2(3H)-thione (6e). White solid, mp 86°C, *R_f* 0.46 (ethyl acetate–hexane, 30 : 70). IR spectrum, ν , cm⁻¹: 3063 [ν (=CH)], 2928, 2838 [ν (CH)], 1675 [ν (C=C)], 1485 [ν (C=N)], 1163, 1093 [ν (COC)]. ¹H NMR spectrum (500 MHz, CDCl₃), δ , ppm: 3.41–3.36 m (4H, CH₂), 4.40 s (2H, NCH₂), 7.42–7.30 m (10H_{arom}), 7.57 d.d (2H_{arom}, *J* 8.2 Hz), 7.61 d.d (2H_{arom}, *J* 8.2 Hz). ¹³C NMR spectrum (125 MHz, CDCl₃), δ , ppm: 23.07, 24.91, 34.75, 114.54, 126.49, 127.05, 127.07, 128.21, 128.33, 128.55, 129.34, 129.21, 129.56, 130.50, 131.52, 132.55, 135.46, 146.76, 158.55, 160.57, 163.41, 167.25. Mass-spectrum, *m/z*: 474.0 [*M* + H]⁺, 476.0 [*M* + 1]⁺. Found, %: C 65.46; H 4.22; N 8.79; S 6.12. C₂₆H₂₀ClN₃O₂S. Calculated, %: C 65.89; H 4.25; N 8.87; S 6.77.

5-[2-(4,5-Diphenyloxazol-2-yl)ethyl]-3-methyl-1,3,4-oxadiazole-2(3H)-thione (6f). White solid, mp 80°C, *R_f* 0.35 (ethyl acetate–hexane, 30 : 70). IR spectrum, ν , cm⁻¹: 3054 [ν (=CH)], 2926, 2863 [ν (CH)], 1670 [ν (C=S)], 1593 [ν (C=C)], 1484 [ν (C=N)], 1166, 1051 [ν (COC)]. ¹H NMR spectrum (300 MHz, CDCl₃), δ , ppm: 2.70 s (3H, CH₃), 3.50–3.30 m (4H, CH₂), 7.42–

7.31 m (6H_{arom}), 7.59 d.d (4H_{arom}, *J* 8.2 Hz). ¹³C NMR spectrum (125 MHz, CDCl₃), δ, ppm: 14.55, 23.03, 25.02, 126.51, 127.90, 127.96, 128.18, 128.61, 128.69, 128.77, 128.90, 129.04, 129.93, 132.26, 133.13, 135.21, 145.77, 160.63, 165.41, 166.33. Mass-spectrum, *m/z*: 364.0 [*M* + 1]⁺. Found, %: C 66.94; H 4.92; N 11.86; O 8.42; S 8.71. C₂₀H₁₇N₃O₂S. Calculated, %: C 66.10; H 4.71; N 11.56; O 8.80; S 8.82.

5-[2-(4,5-Diphenyloxazol-2-yl)ethyl]-3-ethyl-1,3,4-oxadiazole-2(3*H*)-thione (6g). White solid, mp 90°C, *R_f* 0.40 (ethyl acetate–hexane, 30 : 70). IR spectrum, ν, cm⁻¹: 3052 [ν(=CH)], 2927, 2863 [ν(CH)], 1576 [ν(C=C)], 1452 [ν(C=N)], 1269, 1111 [ν(COC)]. ¹H NMR spectrum (400 MHz, CDCl₃), δ, ppm: 1.45 t (3H, CH₃, *J* 7.3 Hz), 3.23 q (2H, NCH₂, *J* 7.3 Hz), 3.45–3.35 m (4H, CH₂), 7.40–7.30 m (6H_{arom}), 7.56 d.d (2H_{arom}, *J* 8.2 Hz), 7.62 d.d (2H_{arom}, *J* 8.2 Hz). ¹³C NMR spectrum (100 MHz, CDCl₃), δ, ppm: 14.68, 22.99, 25.01, 26.89, 126.46, 127.84, 128.11, 128.54, 128.62, 128.73, 132.23, 135.16, 145.70, 160.57, 164.63, 166.14. Mass-spectrum, *m/z*: 378.12 [*M* + 1]⁺. Found, %: C 66.51; H 5.82; N 11.44, O 9.08; S 8.23. C₂₁H₁₉N₃O₂S. Calculated, %: C 66.82; H 5.07; N 11.13; O 8.48; S 8.49.

5-[2-(4,5-Diphenyloxazol-2-yl)ethyl]-3-propyl-1,3,4-oxadiazole-2(3*H*)-thione (6h). White solid, mp 89°C, *R_f* 0.43 (ethyl acetate–hexane, 30 : 70). IR spectrum, ν, cm⁻¹: 3058 [ν(=CH)], 2964, 2871 [ν(CH)], 1581 [ν(C=C)], 1482 [ν(C=N)], 1152, 1061 [ν(COC)]. ¹H NMR spectrum (500 MHz, CDCl₃), δ, ppm: 1.03 t (3H, CH₃, *J* 7.3 Hz), 1.81 m (2H, SCH₂CH₂), 3.19 t (2H, NCH₂, *J* 7.3 Hz), 3.44–3.33 m (4H, CH₂), 7.40–7.29 m (6H_{arom}), 7.56 d.d (2H_{arom}, *J* 8.2 Hz), 7.62 d.d (2H_{arom}, *J* 8.2 Hz). ¹³C NMR spectrum (125 MHz, CDCl₃), δ, ppm: 12.94, 22.50, 22.81, 24.81, 34.22, 126.29, 127.67, 127.95, 128.36, 128.46, 128.58, 132.08, 134.99, 145.52, 160.45, 164.65, 165.96. Mass-spectrum, *m/z*: 392.0 [*M* + 1]⁺. Found, %: C 67.76; H 5.60; N 10.92; S 8.02. C₂₁H₁₉N₃O₂S. Calculated, %: C 67.50; H 5.41; N 10.73; S 8.19.

3-Butyl-5-[2-(4,5-diphenyloxazol-2-yl)ethyl]-1,3,4-oxadiazole-2(3*H*)-thione (6i). Light yellow solid, mp 76°C, *R_f* 0.48 (ethyl acetate–hexane, 30 : 70). IR spectrum, ν, cm⁻¹: 3052 [ν(=CH)], 3002, 2953 [ν(CH)], 1736 [ν(C=S)], 1583, 1495 [ν(C=C)], 1435 [ν(C=N)], 1227, 1167 [ν(COC)]. ¹H NMR spectrum (300 MHz, CDCl₃), δ, ppm: 1.64 t (3H, CH₃, *J* 7.3 Hz), 2.24–2.12 m (4H, SCH₂CH₂), 3.50–3.32 m (4H, CH₂), 3.98 t

(2H, NCH₂, *J* 7.3 Hz), 7.43–7.29 m (6H_{arom}), 7.56 d.d (2H_{arom}, *J* 8.2 Hz), 7.62 d.d (2H_{arom}, *J* 8.2 Hz). ¹³C NMR spectrum (125 MHz, CDCl₃), δ, ppm: 19.23, 22.03, 26.53, 29.42, 35.98, 44.06, 114.71, 122.41, 123.09, 126.01, 126.84, 129.18, 131.48, 136.99, 137.56, 140.06, 143.92, 148.45, 162.56, 170.04. Mass-spectrum, *m/z*: 406.15 [*M* + 1]⁺. Found, %: C 68.91; H 6.07; N 10.93; S 8.06. C₂₃H₂₃N₃O₂S. Calculated, %: C 68.12; H 5.72; N 10.36; S 7.91.

5-[2-(4,5-Diphenyloxazol-2-yl)ethyl]-3-octyl-1,3,4-oxadiazole-2(3*H*)-thione (6j). White solid, mp 86°C, *R_f* 0.53 (ethyl acetate–hexane, 30 : 70). IR spectrum, ν, cm⁻¹: 3063 [ν(=CH)], 2958, 2926 [ν(CH)], 1605 [ν(C=S)], 1594 [ν(C=C)], 1484 [ν(C=N)], 1156, 1063 [ν(COC)]. ¹H NMR spectrum (300 MHz, CDCl₃), δ, ppm: 0.85–0.82 m (8H, CH₂), 1.64–1.57 t (3H, CH₃, *J* 7.0 Hz), 1.81–1.78 t (2H, CH₂, *J* 7.0 Hz), 2.50–2.38 m (2H, CH₂), 3.34 s (2H, CH₂), 4.47–4.42 t (2H, NCH₂, *J* 7.3 Hz), 4.65 s (2H, NCH₂), 7.87–7.80 m (2H_{arom}), 7.97–7.93 t (1H_{arom}, *J* 7.5 Hz), 8.23–8.21 d (1H_{arom}, *J* 8.0 Hz), 8.79 s (1H_{arom}). ¹³C NMR spectrum (125 MHz, CDCl₃), δ, ppm: 19.26, 22.06, 26.41, 29.44, 36.00, 44.08, 125.03, 125.46, 126.88, 127.53, 128.90, 129.23, 131.19, 134.34, 137.60, 140.12, 143.09, 143.94, 162.54, 170.07. Mass-spectrum (ESI-MS), *m/z*: 462.0 [*M* + 1]⁺. Found, %: C 70.91; H 6.62; N 8.84; S 7.01. C₂₇H₃₁N₃O₂S. Calculated, %: C 70.25; H 6.77; N 9.10; S 6.95.

3-Isobutyl-5-[2-(4,5-diphenyloxazol-2-yl)ethyl]-1,3,4-oxadiazole-2(3*H*)-thione (6k). Yellow solid, mp 81°C, *R_f* 0.40 (ethyl acetate–hexane, 30 : 70). IR spectrum, ν, cm⁻¹: 3003 [ν(=CH)], 2924, 2784 [ν(CH)], 1686 [ν(C=S)], 1495 [ν(C=N)], 1225, 1093 [ν(COC)]. ¹H NMR spectrum (300 MHz, CDCl₃), δ, ppm: 1.03 d (6H, CH₃, *J* 6.7 Hz), 2.13–1.95 m (1H, CH), 3.12 d (2H, NCH₂, *J* 6.7 Hz), 3.47–3.30 m (4H, CH₂), 7.41–7.28 m (6H_{arom}), 7.56 d.d (2H_{arom}, *J* 7.4 Hz), 7.62 d.d (2H_{arom}, *J* 7.4 Hz). ¹³C NMR spectrum (125 MHz, CDCl₃), δ, ppm: 14.50, 21.71, 23.02, 25.06, 31.22, 32.22, 126.52, 127.90, 128.27, 128.60, 128.58, 128.79, 132.28, 136.22, 146.76, 162.67, 163.95, 166.28. Mass-spectrum, *m/z*: 406.15 [*M* + H]⁺. Found, %: C 69.42; H 6.01; N 10.83; S 8.05. C₂₃H₂₃N₃O₂S. Calculated, %: C 68.12; H 5.72; N 10.36; S 7.91.

3-Allyl-5-[2-(4,5-diphenyloxazol-2-yl)ethyl]-1,3,4-oxadiazole-2(3*H*)-thione (6l). Yellow solid, mp 72°C, *R_f* 0.43 (ethyl acetate–hexane, 30 : 70). IR

spectrum, ν , cm^{-1} : 3059 [$\nu(\text{=CH})$], 2926, 2856 [$\nu(\text{CH})$], 1583 [$\nu(\text{C=C})$], 1481 [$\nu(\text{C=N})$], 1161, 1059 [$\nu(\text{COC})$]. ^1H NMR spectrum (300 MHz, CDCl_3), δ , ppm: 3.31–3.49 m (4H, CH_2), 3.84 d (2H, NCH_2 , J 6.7 Hz), 5.19 d (1H, CH=CH_2 , J 9.8 Hz), 5.35 d (1H, CH=CH_2 , J 17.3 Hz), 6.10–5.86 m (1H, CH), 7.44–7.30 m (6H_{arom}), 7.56 d.d (2H_{arom} , J 7.5 Hz), 7.62 d.d (2H_{arom} , J 7.5 Hz). ^{13}C NMR spectrum (125 MHz, CDCl_3), δ , ppm: 23.03, 24.98, 35.16, 119.72, 126.53, 127.91, 128.18, 128.61, 128.69, 131.70, 132.27, 135.22, 145.78, 160.61, 164.06, 166.45. Mass-spectrum, m/z : 390.12 [$M+1$] $^+$. Found, %: C 67.44; H 4.12; N 10.43; S 8.36. $\text{C}_{22}\text{H}_{19}\text{N}_3\text{O}_2\text{S}$. Calculated, %: C 67.84; H 4.92; N 10.79; S 8.23.

5-[2-(4,5-Diphenyloxazol-2-yl)ethyl]-3-(prop-2-yn-1-yl)-1,3,4-oxadiazole-2(3H)-thione (6m). White solid, mp 75°C , R_f 0.40 (ethyl acetate–hexane, 30 : 70). IR spectrum, ν , cm^{-1} : 3073 [$\nu(\text{=CH})$], 2923, 2771 [$\nu(\text{CH})$], 2274 [$\nu(\text{C=C})$], 1624 [$\nu(\text{C=S})$], 1509 [$\nu(\text{C=C})$], 1154, 1058 [$\nu(\text{COC})$]. ^1H NMR spectrum (300 MHz, CDCl_3), δ , ppm: 2.29 s (1H, $\equiv\text{CH}$), 3.33–3.51 m (4H, CH_2CH_2), 3.98 s (2H, CH_2), 7.42–7.30 m (6H_{arom}), 7.56 d.d (2H_{arom} , J 7.4 Hz), 7.62 d.d (2H_{arom} , J 7.4 Hz). ^{13}C NMR spectrum (125 MHz, CDCl_3), δ , ppm: 21.02, 23.03, 24.95, 72.99, 76.76, 126.53, 127.90, 128.19, 128.62, 128.70, 128.76, 132.25, 135.23, 145.80, 160.54, 162.98, 166.85. Mass-spectrum, m/z : 388.11 [$M+1$] $^+$. Found, %: C 68.46; H 4.81; N 11.01; S 8.73. $\text{C}_{22}\text{H}_{17}\text{N}_3\text{O}_2\text{S}$. Calculated, %: C 68.20; H 4.42; N 10.85; S 8.28.

CONCLUSIONS

To conclude, 3,5-disubstituted 1a,3,4-oxadiazole derivatives were prepared and evaluated for in vitro anticancer activity against human prostate carcinoma and human lung adenocarcinoma cell lines. Compounds **6b**, **6d**, **6f**, and **6i** showed the highest anticancer activity against the PPC-1 and HTB-57 cell lines with an excellent % inhibition. The designed products showed suitable molecular docking properties and are expected to present a good bioavailability profile. Compound **6f**, **6g**, and **6h** showed the highest binding energies of -7.8 , -7.6 , and -6.8 kcal/mol with Leu431, Leu556, Leu431, Phe435, Val439, and Gln200. Compounds **6a**, **6b**, **6c**, **6g**, and **6h** obeyed the Rule of Five, which suggests their good bioavailability profile. The results of the study allowed us to conclude that the synthesized novel oxadiazoles are an interesting object for further experimentation in the field of searching for efficient anticancer agents.

ACKNOWLEDGMENTS

The authors are highly grateful to the management of the United States Pharmacopeial Convention (USP) for their immense support and motivation for completion of this work. We also extend our gratitude to the management of the Department of Chemistry, KLEF (Deemed to be University) for Ph.D registration.

CONFLICT OF INTEREST

The authors declare no conflict of interest.

REFERENCES

- Bray, F., Ferlay, J., Soerjomataram, I., Siegel, R.L., Torre, L.A., and Jemal, A., *CA: Cancer J. Clin.*, 2018, vol. 68, p. 394. <https://doi.org/10.3322/caac.21492>
- Song, M.X., Zheng, C.J., Deng, X.Q., Sun, L.P., Wua, Y., Hong, L., Li, Y.J., Liu, Y., Wei, Z.Y., Jin, M.J., and Piao, H.R., *Eur. J. Med. Chem.*, 2013, vol. 60, p. 376. <https://doi.org/10.1016/j.ejmech.2012.12.007>
- Liu, Z., Zhao, J., and Huang, X., *Bioorg. Med. Chem. Lett.*, 2006, vol. 16, p. 1828. <https://doi.org/10.1016/j.bmcl.2006.01.002>
- Kumar, K.A., Jayaroopa, P., and Kumar, G.V., *Int. J. Chem. Tech. Res.*, 2012, vol. 4, p. 1782.
- Macaev, F., Ribkovskaia, Z., Pogrebnoi, S., Boldescu, V., Rusu, G., Shvets, N., Dimoglo, A., Geronikaki, A., and Reynolds, R., *Bioorg. Med. Chem.*, 2011, vol. 19, p. 6792. <https://doi.org/10.1016/j.bmc.2011.09.038>
- Jha, K.K., Samad, A., Kumar, Y., Shaharyar, M., Khosa, R.L., Jain, J., Kumar, V., and Singh, P., *Eur. J. Med. Chem.*, 2010, vol. 45, p. 4963. <https://doi.org/10.1016/j.ejmech.2010.08.003>
- Zhang, F., Wang, X.L., Shi, J., Wang, S.F., Yin, Y., Yang, Y.S., Zhang, W.M., and Zhu, H.L., *Bioorg. Med. Chem.*, 2014, vol. 22, p. 468. <https://doi.org/10.1016/j.bmc.2013.11.004>
- Rajak, H., Singh, T.B., Singh, A., Raghuvanshi, K., Sah, A.K., Veerasamy, R., Sharma, P.C., Singh, P.R., and Kharya, M.D., *Bioorg. Med. Chem. Lett.*, 2013, vol. 23, p. 864. <https://doi.org/10.1016/j.bmcl.2012.11.051>
- Sangshetti, J.N., Chabukswar, A.R., and Shinde, D.B., *Bioorg. Med. Chem. Lett.*, 2011, vol. 21, p. 444. <https://doi.org/10.1016/j.bmcl.2010.10.120>
- Ramaprasad, G.C., Kalluraya, B., Kumar, B.S., and Hunnur, R.K., *Eur. J. Med. Chem.*, 2010, vol. 45, p. 4587. <https://doi.org/10.1016/j.ejmech.2010.07.021>

11. Ziedan, N.I., Stefanelli, F., Fogli, S., and Westwell, A.D., *Eur. J. Med. Chem.*, 2010, vol. 45, p. 4523.
<https://doi.org/10.1016/j.ejmech.2010.07.012>
12. Manjunatha, K., Poojary, B., Lobo, P.L., Fernandes, J., and Kumari, N.S., *Eur. J. Med. Chem.*, 2010, vol. 45, p. 5225.
<https://doi.org/10.1016/j.ejmech.2010.08.039>
13. Wang, Y., Xie, Y., and Oupicky, D., *Curr. Pharmacol. Rep.*, 2016, vol. 2, p. 1.
<https://doi.org/10.1007/s40495-015-0044-8>
14. Jakopin, Z. and Dolenc, M.S., *Curr. Org. Chem.*, 2008, vol. 12, p. 850.
<https://doi.org/10.2174/138527208784911860>
15. Tang, J.F., Lv, X.H., Wang, X.L., Sun, J., Zhang, Y.B., Yang, Y.S., Gong, H.B., and Zhu, H.L., *Bioorg. Med. Chem.*, 2012, vol. 20, p. 4226.
<https://doi.org/10.1016/j.bmc.2012.05.055>
16. Farand, J., Mai, N., Chandrasekhar, J., Newby, Z.E., Van Veldhuizen, J., Loyer-Drew, J., Venkataramani, C., Guerrero, J., Kwok, A., Li, N., Zherebina, Y., Wilbert, S., Zablocki, J., Phillips, G., Watkins, W.J., Mourey, R., and Notte, G.T., *Bioorg. Med. Chem. Lett.*, 2016, vol. 26, p. 5926.
<https://doi.org/10.1016/j.bmcl.2016.10.092>
17. <http://www.molinspiration.com>
18. Lipinski, C.A., Lombardo, F., Dominy, B.W., and Feeney, P.J., *Adv. Drug Delivery Rev.*, 1997, vol. 23, p. 3.
[https://doi.org/10.1016/S0169-409X\(96\)00423-1](https://doi.org/10.1016/S0169-409X(96)00423-1)
19. Gerlier, D. and Thomasset, N., *J. Immunol. Methods*, 1986, vol. 94, p. 57.
[https://doi.org/10.1016/0022-1759\(86\)90215-2](https://doi.org/10.1016/0022-1759(86)90215-2)
20. Abu Bakar, M.F., Maryati, M., Rahmat, A., Burr, S.A., and Fry, J.R., *Food Chem. Toxicol.*, 2010, vol. 48, p. 1688.
<https://doi.org/10.1016/j.fct.2010.03.046>
21. Morris, G.M., Huey, R., Lindstrom, W., Sanner, M.F., Belew, R.K., Goodsell, D.S., and Olson, A.J., *J. Comput. Chem.*, 2009, vol. 16, p. 2785.
<https://doi.org/10.1002/jcc.20256>
22. Banu, S., Bollu, R., Nagarapu, L., Nanubolu, J.B., Yogeswari, P., and Sriram, D., *Chem. Biol. Drug Des.*, 2018, vol. 92, p. 1315.
<https://doi.org/10.1111/cbdd.13196>
23. Laskowski, R.A., *Nucleic Acids Res.*, 2009, vol. 37, p. 355.
<https://doi.org/10.1093/nar/gkn860>